

Propagation and Selective Transmission of Internal Gravity Waves in a Sudden Warming¹

TIMOTHY J. DUNKERTON

Physical Dynamics, Inc., Bellevue, WA 98009

NEAL BUTCHART

Department of Atmospheric Sciences, University of Washington, Seattle, WA 98195

(Manuscript received 19 September 1983, in final form 19 January 1984)

ABSTRACT

Longitudinally asymmetric features of gravity wave propagation in a sudden warming are examined theoretically, using observed geostrophic wind fields in the stratosphere for three days of winter 1979. It is shown that the wind patterns accompanying a sudden warming act to reduce, but not eliminate, quasi-stationary gravity wave propagation to the mesosphere. The onset of large-amplitude planetary waves leads to the formation of propagating zones and forbidden zones for gravity waves of intermediate horizontal scale (50–200 km). Lateral ray movement and horizontal refraction are secondary but observable effects for these waves.

To the extent that these waves are excited isotropically in the troposphere, it is possible to evaluate the direction and magnitude of the average wavevector reaching the mesosphere as follows. Stationary waves with wavevector orthogonal to the local mean flow are selectively absorbed in the stratosphere, implying that for these waves the average wavevector transmitted to the mesosphere is antiparallel to the average of the mean flow orientation extrema in the underlying stratosphere.

1. Introduction

Vertically propagating internal gravity waves are thought to transport momentum from the lower to upper atmosphere, accelerating the upper level mean flow regions of wavebreaking (Lindzen, 1981; Holton, 1982), dissipation (Matsuno, 1982) and critical layer absorption (Dunkerton, 1982a,b). Such accelerations appear to be required in the winter mesosphere to balance Coriolis torques due to the mean meridional circulation (Leovy, 1964; Schoeberl and Strobel, 1978; Holton and Wehrbein, 1980; Lindzen, 1981; Holton, 1982). Radar observations now suggest that gravity waves are able to retard the mean flow in this manner (Vincent and Reid, 1983).

As Lindzen (1981) and Matsuno (1982) have elucidated, the concept of selective transmission is crucial to the behavior of vertically propagating internal gravity waves. For quasi-stationary waves with phase speed much less than the mean flow speed, wavevectors that become aligned orthogonal to the local or phase-averaged mean flow are selectively absorbed and cannot propagate vertically through the critical level (Bretherton, 1966). This suggests, for example, that quasi-stationary waves of zonal orientation are trapped by critical levels in the transition region from tropospheric westerlies to summer stratospheric easterlies, and can-

not reach the mesosphere in this season. In winter, on the other hand, such waves are free to propagate vertically in westerly winds; this appears to explain why gravity wave activity is more pronounced in the winter mesosphere (Lindzen, 1981).

Vertical propagation of quasi-stationary gravity waves is believed to diminish, however, during a sudden stratospheric warming. In the Northern Hemisphere, the zonal mean flow is westerly in winter during quiescent periods, but reverts to easterly at high latitudes in a major warming. Recognizing this, Lindzen (1981) and Holton (1983) have suggested that the appearance of easterlies will inhibit propagation of quasi-stationary gravity waves to the mesosphere. Their conclusion is correct insofar as a sudden warming will reduce the horizontal extent of the propagating regions. However, the situation is complicated by the presence of planetary waves. In winter, there may temporarily exist regions of local easterlies, here and there, where vertical propagation of zonal quasi-stationary waves is inhibited. During a sudden warming, on the other hand, there will certainly exist regions of local westerlies in which such propagation is allowed. In both cases, the selective transmission of gravity waves will become a function of *longitude* whenever and wherever planetary wave winds are comparable in amplitude to the zonal mean flow (Dunkerton, 1982b; Schoeberl and Strobel, 1983).

The presence of planetary waves implies, moreover, a significant meridional component of the local mean flow. This component will affect the transmission of

¹ Contribution No. 695, Department of Atmospheric Sciences, University of Washington.

gravity waves, determining which wavevector orientations encounter critical levels. The results can differ greatly from those of a zonally symmetric zonal flow; note, for example, that stationary waves of meridional orientation, which might be excited by an east-west mountain range, are allowed to propagate vertically in the presence of planetary waves.

Clearly, then, planetary waves must be taken into account if we are to assess how sudden warmings and other mean flow variations will affect the vertical propagation of internal gravity waves in the winter stratosphere. The purpose of this paper is to attempt such an assessment, based on actual observations of geostrophic winds in the Northern Hemisphere winter. This will be done by solving the ray tracing equations for internal gravity waves for three days of winter 1979: a "normal" day (17 January), a "minor" wave 1 warming (26 January), and a major wave 2 warming (22 February). Satellite-derived geostrophic wind fields are then used in a numerical model to assess changes in gravity wave propagation brought about by these two sudden warmings. In this paper, attention will be restricted to gravity waves of the "intermediate" range (50–200 km) for which nonhydrostatic and Coriolis effects are small. The importance of these waves in the mesospheric momentum budget has been established by the radar observations of Vincent and Reid (1983). Because their radar technique is biased towards these smaller scales, it would be premature to exclude larger-scale inertia-gravity waves from the momentum budget. Such waves are observed in the mesosphere (Smith and Fritts, 1983), but their importance cannot yet be assessed. As part of an ongoing project, we are now beginning to examine these larger-scale waves theoretically (Dunkerton, 1984). In the meantime, it is of interest to examine the behavior of the intermediate-scale waves, for which the greatest degree of simplification is possible. These waves move rapidly in the vertical, and experience rather small lateral displacement and refraction (Jones, 1969).

Based on the results of this study, it will become apparent that 1) longitudinal asymmetries in gravity wave transmission exist throughout the Northern Hemisphere winter, but especially during a sudden warming; 2) zones of significant quasi-stationary gravity wave propagation exist even in a major warming; and 3) the average transmitted wavevector for these waves lies within the range of orientations permitted by the lower-level flow, implying that for an isotropic initial distribution and a conservative flow away from critical levels, the average transmitted wavevector is antiparallel to the average of the mean flow orientation extrema in the underlying stratosphere.

These results are attributable to the principle of selective transmission and the approximately equivalent barotropic character of the sudden warming. Stationary waves having a nonzero wavevector component an-

tiparallel² to the local mean flow survive and propagate vertically, while orthogonal waves are selectively absorbed in the stratosphere (Matsuno, 1982).

To illustrate these previously unrecognized features of selective transmission in a sudden warming, it will be assumed, following Matsuno (1982), that gravity waves of all orientations are excited isotropically in the troposphere. The results to be presented here will then represent an upper limit on the amount of quasi-stationary gravity wave action that can be transmitted through the longitudinally asymmetric stratosphere. In Section 2, the ray tracing equations are discussed, together with the numerical model used to solve them. Sections 3 and 4 present geostrophic wind fields and ray tracing results, respectively, for three days of winter 1979. Finally, Section 5 describes a simplified approach valid when lateral movement and horizontal refraction can be ignored. This method yields an economical estimate of the distribution of gravity waves reaching the stratopause, which confirms the overall patterns obtained by ray tracing in the small horizontal wavelength limit.

2. The ray tracing problem

a. Gravity waves in the "intermediate" range

Waves in the intermediate range satisfy

$$f \ll |\hat{\omega}| \ll N, \quad (2.1)$$

where f is the Coriolis parameter (10^{-4} s^{-1}), $\hat{\omega}$ is intrinsic frequency, and N is the static stability (0.02 s^{-1}). For various horizontal scales λ_x , (2.1) requires that

$$\left. \begin{aligned} 0.16 \text{ m s}^{-1} \ll |\hat{c}| \ll 32 \text{ m s}^{-1} & \quad (\lambda_x = 10 \text{ km}) \\ 1.6 \text{ m s}^{-1} \ll |\hat{c}| \ll 320 \text{ m s}^{-1} & \quad (\lambda_x = 100 \text{ km}) \\ 16 \text{ m s}^{-1} \ll |\hat{c}| \ll 3200 \text{ m s}^{-1} & \quad (\lambda_x = 1000 \text{ km}) \end{aligned} \right\}, \quad (2.2)$$

where \hat{c} is the intrinsic phase speed. For typical stratospheric values lying in the range $0 < |\hat{c}| < 100 \text{ m s}^{-1}$, the short waves will not be hydrostatic, and may be evanescent in the polar night jet, whereas the long waves will be affected by rotation. Jones (1967) has argued that under conservative conditions gravity waves are always affected by rotation before encountering their critical level ($\hat{c} = 0$). We prefer to adopt the view that rotation will become important in this limit only if wavebreaking or dissipation have not yet become important as $\hat{c} \rightarrow 0$. The importance of rotation will be suppressed by the turbulent cascade to higher wavenumbers in the case of wavebreaking, while dis-

² The orientation of a gravity wave is defined by its wavevector, orthogonal to wave crests. It is strictly a matter of convention whether waves are labeled "parallel" or "antiparallel" relative to the mean flow; all possible horizontal orientations lie within a semi-circle (Matsuno, 1982).

sipated waves will not survive long enough for rotation to be of any consequence (see Appendix to Jones, 1967). In a conservative linear shear flow, it can be shown that direct convective wavebreaking will occur long before $|\hat{\omega}| \rightarrow |f|$ if

$$|\mathbf{B}_0| \gg \frac{f^3}{2NK^2}, \quad (2.3)$$

where \mathbf{B}_0 is the momentum flux and K is total horizontal wavenumber. It will be assumed that (2.3) is implicitly satisfied, although the ray tracing calculations to be presented here make no reference to wave amplitude.

For a given value of intrinsic phase speed, the concept of an "intermediate" range refers to both frequency and horizontal scale. In this paper, quasi-stationary waves of horizontal scale 50–200 km will be considered to lie within this range. Eq. (2.1) is satisfied by waves having intrinsic periods much greater than 6 min and much less than 18 h.

b. Ray tracing equations

An elegant introduction to ray tracing appears in Lighthill (1978). For waves satisfying a dispersion relation of the form

$$\omega = \omega(k_i, x_i), \quad (2.4)$$

where ω , x_i and k_i are frequency, position and wavevector, respectively, the ray tracing equations assume the general form

$$dx_{ij}/dt = +\partial\omega/\partial k_i, \quad (2.5a)$$

$$dk_{ij}/dt = -\partial\omega/\partial x_i. \quad (2.5b)$$

The time derivative is taken along a ray, which by (2.5a) moves with the group velocity. Eq. (2.5b) describes the refraction of the wavevector along a ray due to inhomogeneities in the basic state. Notably,

$$d\omega/dt = 0, \quad (2.5c)$$

since the basic state is assumed steady.

The hydrostatic limit of Bretherton's (1966) dispersion relation is

$$\hat{\omega} = \omega - \mathbf{k} \cdot \bar{\mathbf{u}} = \pm \frac{NK}{m}, \quad (2.6)$$

where—as throughout our paper— \mathbf{k} and $\bar{\mathbf{u}}$ denote the horizontal component of wavevector and mean flow (whence $K \equiv |\mathbf{k}|$). The vertical wavenumber m is assumed to satisfy a local Boussinesq approximation, i.e.,

$$m^2 \gg O\left(\frac{1}{4H^2}\right), \quad (2.7)$$

where H is the density scale height.

Substitution of (2.6) in (2.5a,b) implies

$$dx/dt \equiv \mathbf{u}_g = \bar{\mathbf{u}} + \mathbf{k}^* \hat{c}, \quad (\mathbf{k}^* \equiv \mathbf{k}K^{-1}), \quad (2.8a)$$

$$dz/dt \equiv w_g = K\hat{c}^2/N, \quad (\hat{c} = \hat{\omega}k^{-1}), \quad (2.8b)$$

$$dk_{ij}/dt = -k_j \partial \bar{u}_j / \partial x_i, \quad (i = 1, 2), \quad (2.8c)$$

where x and z are horizontal and vertical position, \mathbf{u}_g is the horizontal component of the group velocity, and w_g is the vertical group velocity, assumed positive. The basic state is assumed temporally constant, and N is taken to be spatially constant as well. Steadiness of the basic state is appropriate for waves of the intermediate range, but is likely to be less accurate for inertia-gravity waves in the period leading up to a sudden warming. Comparison of (2.8a, b) indicates that the vertical-to-horizontal slope of a ray is proportional to the total horizontal wavenumber. Therefore lateral ray movement will tend to increase with increasing horizontal wavelength. This implies that refraction will have more time to operate at the longer scales.

In this paper the ray tracing calculations have been done on a spherical earth. Effects of the spherical coordinate system are usually negligible for the intermediate-scale waves except very close to the pole. To deal with the artificial geometrical refraction of waves near the pole, the local components of \mathbf{k} were time-stepped with the necessary terms added to the right-hand side of (2.8c) to insure great circle propagation in a resting basic state (Gossard and Hooke, 1975).

c. Stationary waves

The dispersion relation for upward-propagating stationary wave packets is

$$\mathbf{k}^* \cdot \bar{\mathbf{u}} = \frac{N}{m}. \quad (2.9)$$

For these waves,

$$\mathbf{u}_g = \bar{\mathbf{u}} - \mathbf{k}^*(\mathbf{k}^* \cdot \bar{\mathbf{u}}), \quad (2.10a)$$

$$w_g = \frac{K}{N} (\mathbf{k}^* \cdot \bar{\mathbf{u}})^2. \quad (2.10b)$$

Alternately, if

$$\mathbf{k}^* \cdot \bar{\mathbf{u}} \equiv |\bar{\mathbf{u}}| \cos \alpha_r,$$

then

$$|\mathbf{u}_g| = |\bar{\mathbf{u}}| |\sin \alpha_r|, \quad (2.11a)$$

$$w_g = \frac{K |\bar{\mathbf{u}}|^2 \cos^2 \alpha_r}{N}. \quad (2.11b)$$

For stationary waves, $\alpha_r = \pm \pi/2$ is a critical level, where

$$m = \infty, \quad w_g = 0, \quad (2.12a, b)$$

$$\mathbf{k}^* \cdot \bar{\mathbf{u}} = 0, \quad \mathbf{u}_g = \bar{\mathbf{u}}. \quad (2.12c, d)$$

At this point wavebreaking and dissipation become important (e.g., Dunkerton and Fritts, 1984). By (2.12c), one can refer to the stationary wave critical

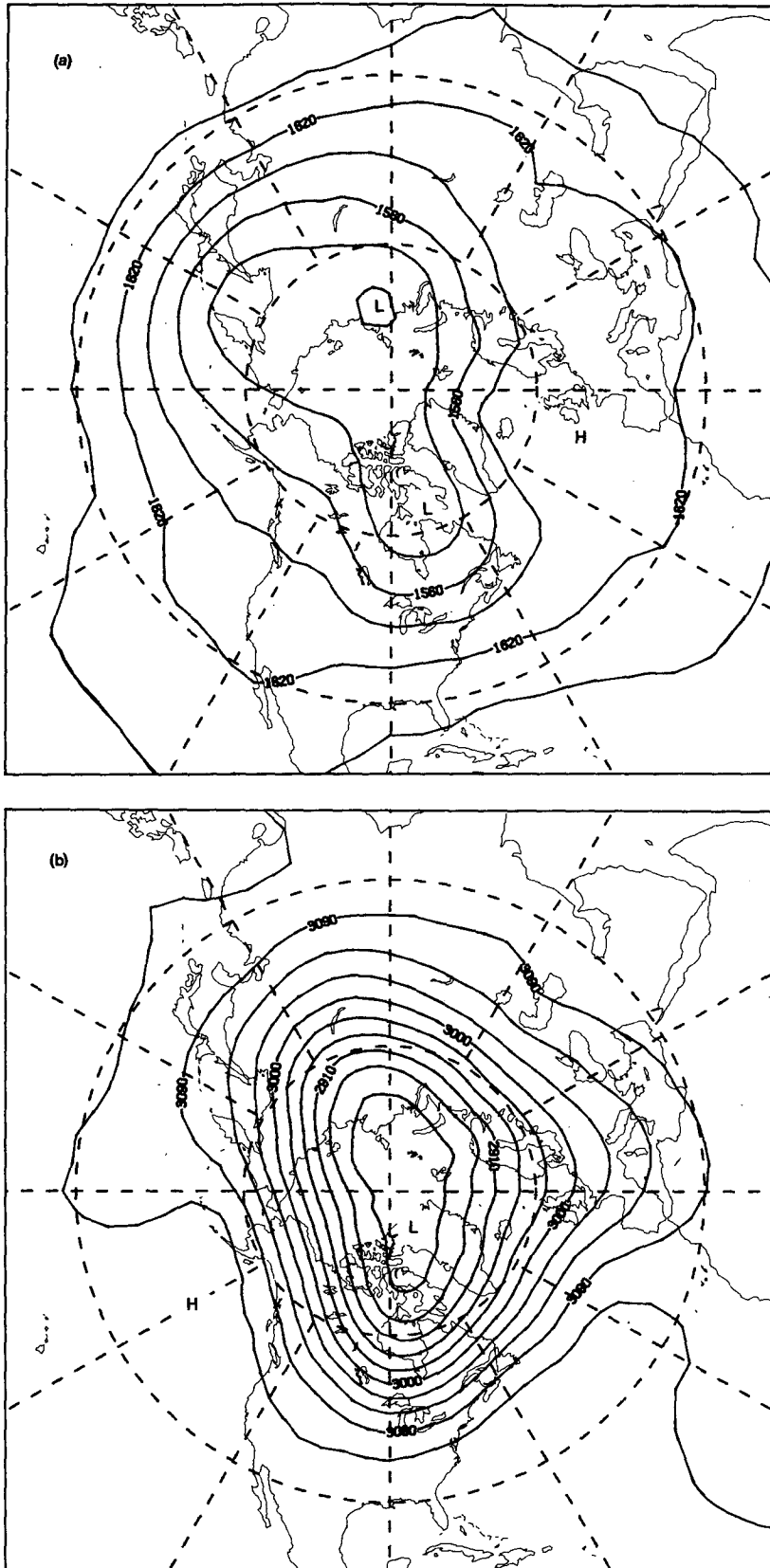


FIG. 1. Geopotential contours (dam) for 17 January 1979:
(a) 100 mb, (b) 10 mb, (c) 1 mb.

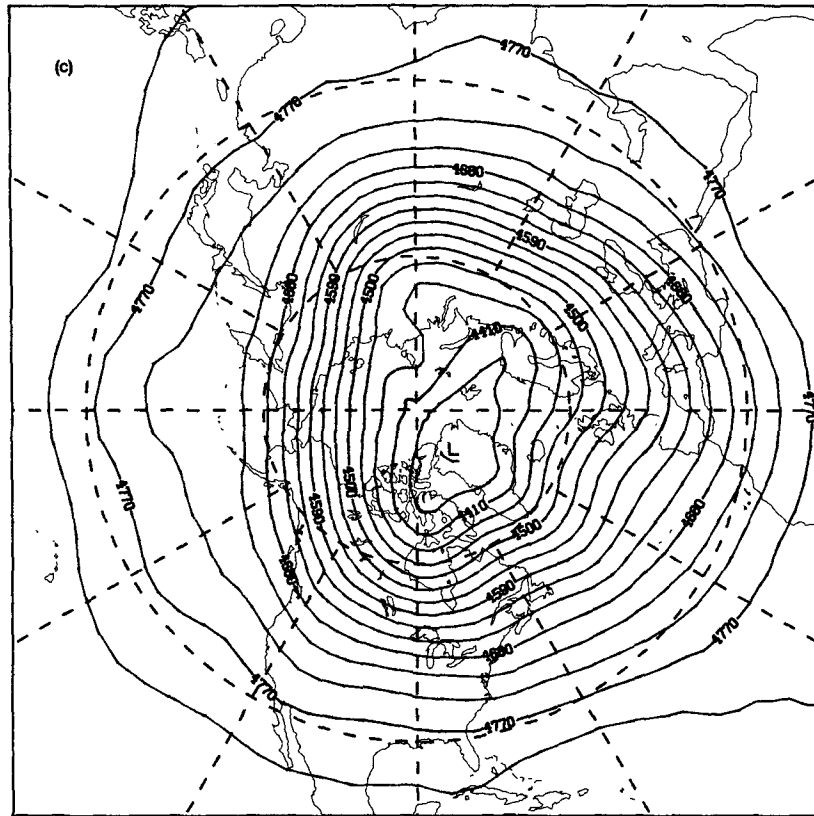


FIG. 1. (Continued)

level as a "point of orthogonality." More generally, whenever the groundbased phase speed is much less than $|\bar{u}|$, the critical level is approximately a point of orthogonality.

Under such circumstances, and for strong geostrophic flow, (2.12c) implies that *quasi-stationary waves are selectively absorbed when their horizontal wavevectors become approximately orthogonal to the local geopotential contours.*

d. Critical damping concept

The ray tracing results of the following section make no reference to wave amplitude or wavebreaking, although we suppose that this could be done in a more ambitious treatment using wave action conservation. To simplify the parameter space, wave amplitude is assumed small, but subject to (2.3).

For intermediate-scale waves, stratospheric dissipation is negligible except in regions of very small intrinsic phase speed. Calculating ray positions in such regions consumes unnecessary computer time, however, since the ray time will be infinite approaching a horizontally homogeneous critical level. The numerical code has therefore been economized by disposing of what are thought to be highly dissipated rays when the spatial divergence of rays is ignored, i.e., rays for which

$$w_g H^{-1} < \alpha_T(m) \quad (2.13)$$

(Dunkerton, 1979). Here, α_T is the wavenumber-dependent radiative damping rate of Fels (1982). In Fels' $m^{1/2}$ regime this implies a critical vertical wavenumber at which point the ray calculation is terminated:

$$m_c = \left(\frac{NK\sqrt{m_0}}{H\alpha_T(m_0)} \right)^{2/5}, \quad (2.14)$$

where $m_0 = 1 \text{ km}^{-1}$.

e. Numerical model

Briefly, the numerical code employs forward differencing and a 1 min time step to advance (2.8a-c) beginning from an initial configuration of 180 rays equally spaced on each of six latitude circles (30–80°N) at 10 km. Each ray is assigned the same parameter values, including the same initial wavevector orientation α_0 relative to the local latitude circle. Geopotential data from the Stratospheric Sounding Unit (SSU) analyses were used to calculate geostrophic winds, and linear interpolation was performed in latitude and height to determine \bar{u} along a ray. In longitude, the lowest three planetary waves were retained from the original data, since these planetary waves contain most of the wind variance in the stratosphere:

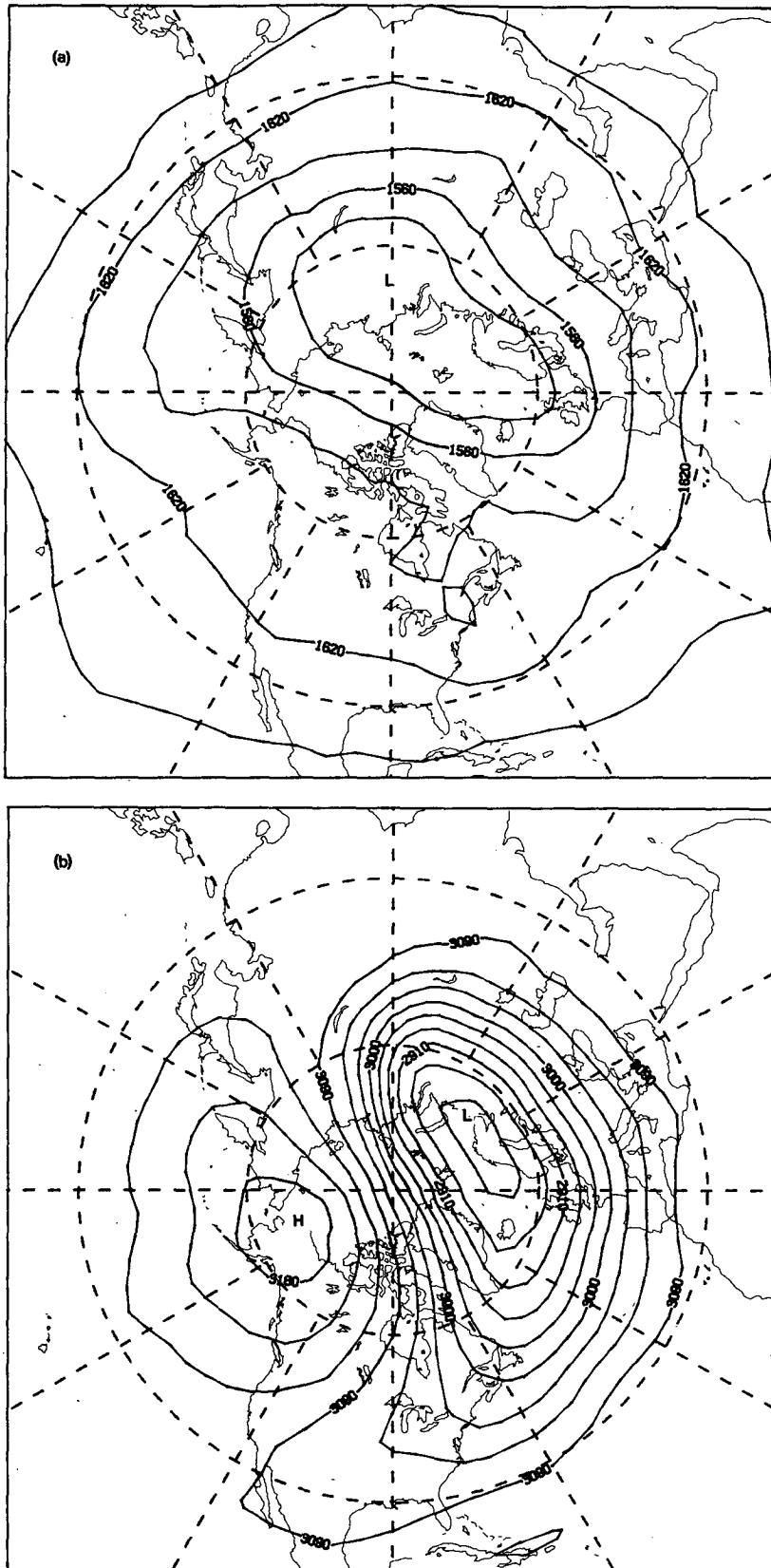


FIG. 2. As in Fig. 1, but for 26 January 1979.

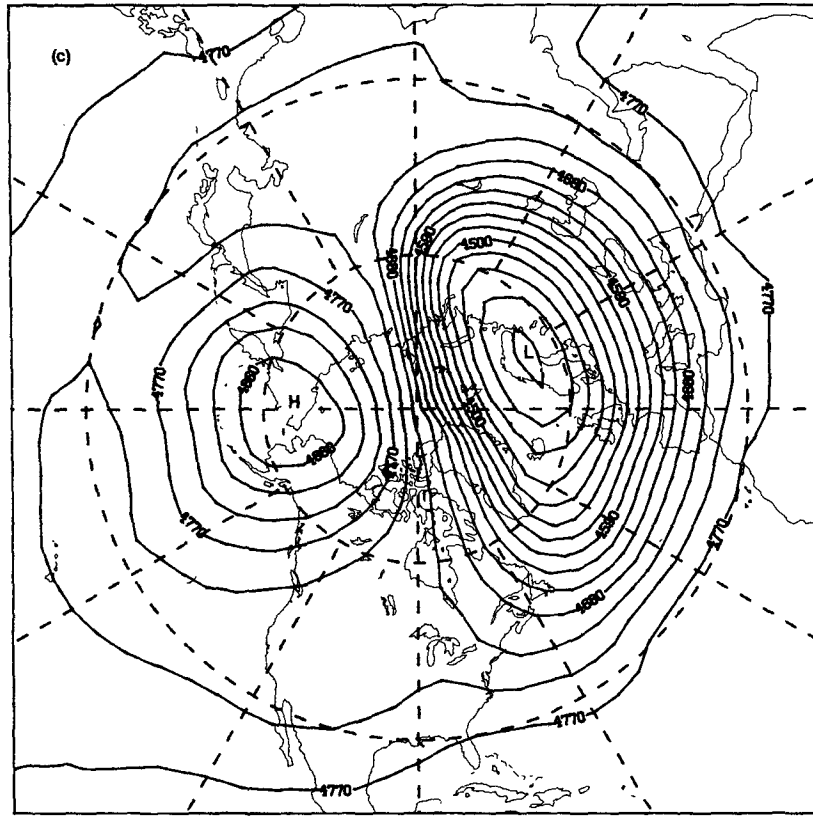


FIG. 2. (Continued)

$$\bar{u}(\lambda, \theta, z) = \bar{u}_0(\theta, z) + \operatorname{Re} \sum_{n=1}^3 \bar{u}_n(\theta, z) \exp i n \lambda, \quad (2.15)$$

where λ and θ are longitude and latitude, respectively. This method is sufficient to obtain the planetary-scale patterns of gravity wave propagation, but it should be mentioned that smaller scale motions, including those due to nearby inertia-gravity waves not detected by satellite, will have local effects on ray propagation.

Ray positions were advanced until $z = 1$ mb, or $m = m_c$, or 48 h had elapsed. In the vicinity of the polar night jet, intermediate-scale waves traverse the entire stratosphere in a matter of one to a few hours. Ray times may exceed 24 h, however, in regions of weak winds. To monitor such waves, the model was integrated into a second day, if necessary, but using wind fields from the first day.

3. Geostrophic wind fields

a. A "normal" day

Early in this investigation it became apparent that day-to-day variations in the flow at the lowest levels of the model would have significant effects on gravity wave propagation. As a result, there is probably no such thing as a truly normal day against which gravity wave propagation in the Northern Hemisphere winter

can be compared. Indeed, tropospheric flow conditions will determine the excitation of gravity waves in the first place.

Having made note of this caveat, Fig. 1 displays geopotential contours at 100, 10 and 1 mb for 17 January 1979 obtained from SSU analyses. This day was fairly undisturbed as far as the upper stratospheric flow was concerned. The polar night jet was distorted by planetary waves, predominantly wave 1 at 1 mb and a mixture of waves 1 and 2 at 100 mb. A deep low over Hudson Bay extended well into the stratosphere, distorting the jet into a highly curved configuration. A shallower low was present over Siberia. Very weak geostrophic winds were observed at 100 mb over Europe, and in an "Aleutian" high from 20 to 5 mb.

b. A "minor" wave 1 warming

On 26 January 1979 a rather simple, and predominantly zonal, flow existed at 100 mb (Fig. 2). But at higher levels the Aleutian high had grown significantly in amplitude, now centered over the Bering Strait. On the opposite side of the hemisphere an unusually strong vortex was centered over northern Scandinavia. This vortex was approximately equivalent barotropic above 20 mb, exhibiting a more significant phase tilt with height only in the lower stratosphere.

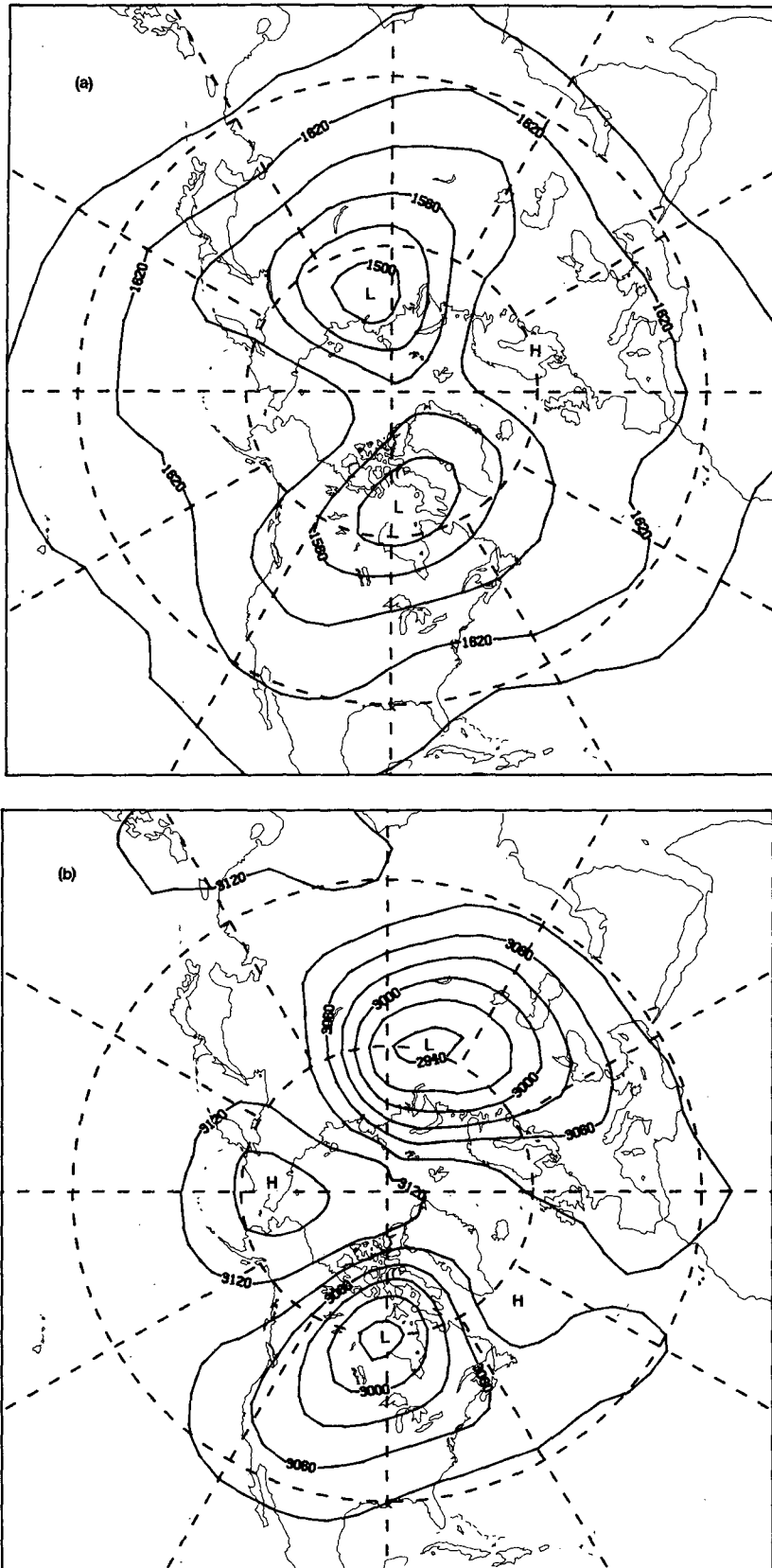


FIG. 3. As in Fig. 1, but for 22 February 1979.

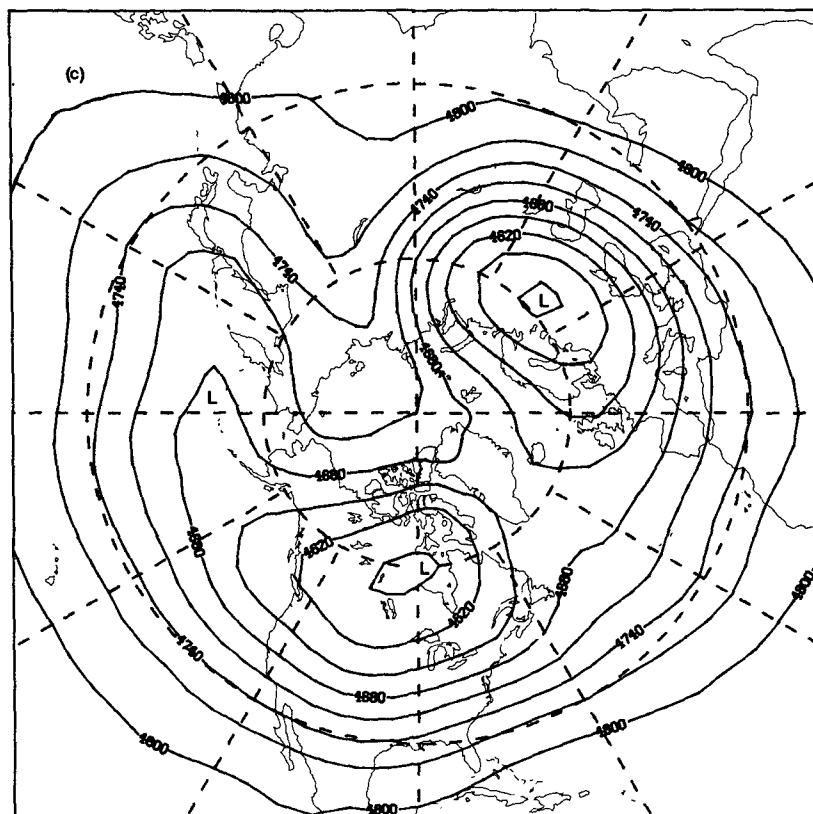


FIG. 3. (Continued)

Convention labels this warming as “minor,” considering the magnitude and depth of the mean temperature increase at high latitudes. The ray tracing results of the next section will establish, however, that this was a major warming from the point of view of gravity waves.

c. A major wave 2 warming

To some extent, the major warming of 22 February 1979 was approximately equivalent barotropic (Fig. 3). There was, however, a 60° phase tilt in the Siberian low, and a strong ridging action towards the pole at 1 mb over eastern Siberia.

Note should be made that for both warmings (Figs. 2 and 3), the zonal mean flow reverted to easterly in the high latitude upper stratosphere, the effect being somewhat more pronounced on 22 February.

4. Ray tracing results and discussion

a. 17 January 1979

On this day the upper stratospheric flow was sufficiently zonally symmetric that quasi-stationary waves could reach the stratopause over much of Fig. 1. Nevertheless, some interesting features appear in the ray

tracing calculations dependent on the 100 mb flow and the initial orientation of the wavevector.

Figure 4 shows “ray contour projections” at the 1 mb surface for the parameters

$$K_0 = 2\pi (100 \text{ km})^{-1} \sqrt{2}, \quad (4.1a)$$

$$\alpha_0 = +45^\circ, \quad (4.1b)$$

$$c = 0, \quad (4.1c)$$

with initial wavevector orientation aligned SW-NE. (Relative to a westerly mean flow, these waves propagate to the southwest.) We have endeavoured to make this and the following figures easy to comprehend, although presenting three-dimensional ray tracing results on a two-dimensional journal page is not a small task. A “ray contour” for our purposes is the locus of points defined by all rays initially lying on the same latitude circle at the start of integration. A “ray contour projection” is the locus of points on the model’s upper boundary (1 mb) where the corresponding ray contour has passed through that surface. The time of arrival at 1 mb is, of course, different for each ray, as is the final wavevector. The final position and orientation of 10 rays on each latitude circle are shown in Fig. 4 (circles). These rays were initially placed at equal longitude intervals (0° , 36° , 72° , etc.).

In general, for waves of the intermediate range a

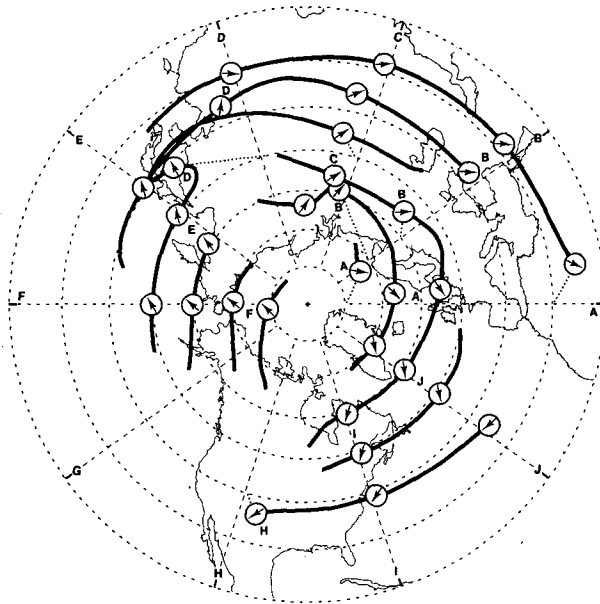


FIG. 4. Ray contour projections on the 1 mb surface for 17 January 1979, for the case $K_0 = 2\pi (100 \text{ km})^{-1} \sqrt{2}$, $\alpha_0 = +45^\circ$, $c = 0$. Circles denote final ray positions for rays initially at equal intervals of 36° (labeled A, B, C, etc.). In a few cases a dotted line connects initial and final position for added clarity. Arrows within circles denote final wavevector orientation (but not magnitude). Antiparallel convention is assumed.

ray contour projection most closely approximates the original position of the corresponding ray contour wherever the vertical slope of the ray is large. On the other hand, lateral movement and horizontal refraction may affect slowly moving rays. On account of critical levels, some rays never reach the stratopause at all, therefore the ray contours and their projections may be broken. For clarity, in this and the following figures a few highly displaced rays have been omitted at the ends of contours, where ray overlapping is sometimes observed.

Figure 4 is somewhat complex, due to longitudinal asymmetries in the mean flow and the choice of a nonzonal orientation. The latter implies that even stationary waves "move" laterally in terms of their group propagation (2.10a) or (2.11a). Nevertheless, an important pattern for quasi-stationary waves appears in Fig. 4, viz., that ray contour projections most closely approximate their initial latitude circles when the mean flow in the stratosphere is most nearly antiparallel to k^* . In this case lateral movement is minimized in regions of southwesterly (SW to NE) winds, notably over northeastern Canada and in an arc extending from $180^\circ, 80^\circ\text{N}$ to the vicinity of $135^\circ, 40^\circ\text{N}$. This flow orientation was also present over the western USSR, but the west-northwesterly flow at 100 mb complicated matters at this point.

At the opposite extreme are regions devoid of these particular waves at 1 mb. Weak winds at 100 mb have obstructed rays over Siberia, northern Canada, and all

of southern Europe. The stratospheric Aleutian high has had a similar effect in that region. Perhaps of most interest is the situation just west of 270° ; here, a strong polar night jet flows southwestward parallel to the Canadian Rockies. Our stationary waves are trying to propagate orthogonal to this flow, however, and cannot reach the stratopause.

Between these two extremes are rays that reach the stratopause after a longer time, having experienced a larger horizontal displacement, and perhaps significant refraction. In general, these rays are more difficult to interpret theoretically. In Fig. 4 lateral ray movement is directed to the southeast in westerlies. However, equatorward of the jet there is an anticyclonic rotation of the wavevector in the anticyclonic shear, so that some rays initially at 30° have begun to propagate to the north. This behavior resembles Jones' (1969) linear temporal variation of the wavevector in a flow where rotation dominates over deformation.

The situation on this day is quite different for stationary waves of identical K_0 , but having an initial NW-SE orientation, i.e.,

$$\alpha_0 = -45^\circ, \quad (4.2)$$

as shown in Fig. 5. Regions of southwesterly (SW to NE) flow are devoid of these waves, whereas some regions in Fig. 4 lacking $+45^\circ$ waves are now covered with -45° waves. Superposition of the two figures considerably increases the extent of coverage by stationary waves at 1 mb; nevertheless, the presence of weak 100 mb flow and a stratospheric "Aleutian" high are still felt at 1 mb.

Comparison of Figs. 4 and 5 suggests that the selective transmission of waves implies a tendency for

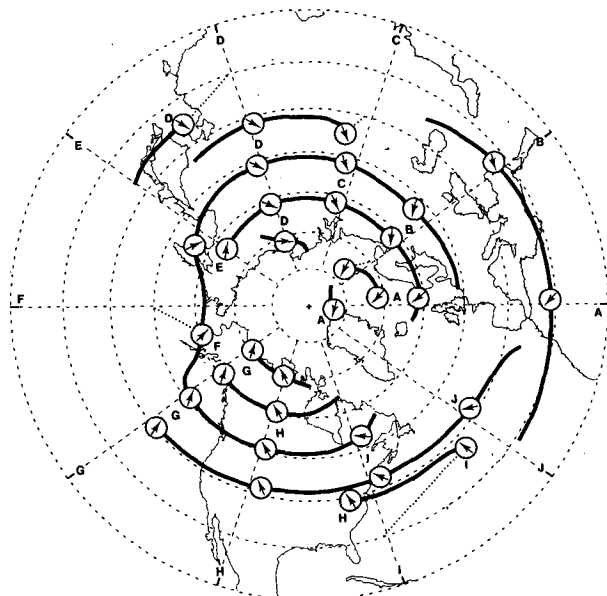


FIG. 5. As in Fig. 4, but with $\alpha_0 = -45^\circ$.

the surviving stationary waves to be oriented antiparallel to the mean flow at 1 mb, to the extent that the flow is approximately equivalent barotropic below this level. This result is strictly a consequence of the selective transmission of vertically-propagating rays; lateral movement and horizontal refraction seem to complicate this simple picture. To be sure, the mean flow is never exactly equivalent barotropic, so that the average transmitted wavevector is never exactly antiparallel to the 1 mb flow. An economical method has been devised in Section 5 for evaluating the direction and magnitude of the average transmitted wavevector when lateral ray movement and horizontal refraction can be neglected, an approximation which holds best for waves of the intermediate range.

b. 26 January 1979

Figure 6 displays ray contour projections for the case

$$K_0 = (200 \text{ km})^{-1} \sqrt{2}, \quad (4.3a)$$

$$\alpha_0 = +45^\circ, \quad (4.3b)$$

$$c = 0, \quad (4.3c)$$

for waves propagating in the geostrophic wind fields of a wave 1 warming (Fig. 2). Propagation is forbidden in northwesterly (NW to SE) or weak winds. Therefore, rays do not reach the stratopause 1) in the strongly curved flow in quadrant IV (270° to 360°); 2) in the middle of the high and low pressure centers; 3) east and south of the Alaskan high, where the wind vector rotates up to 180° with height; and 4) far southwest

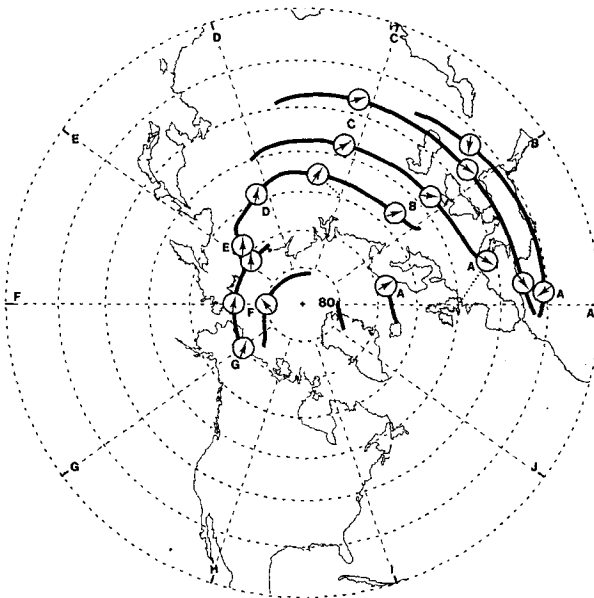


FIG. 6. As in Fig. 4, but for 26 January 1979 and $K_0 = 2\pi (200 \text{ km})^{-1} \sqrt{2}$.

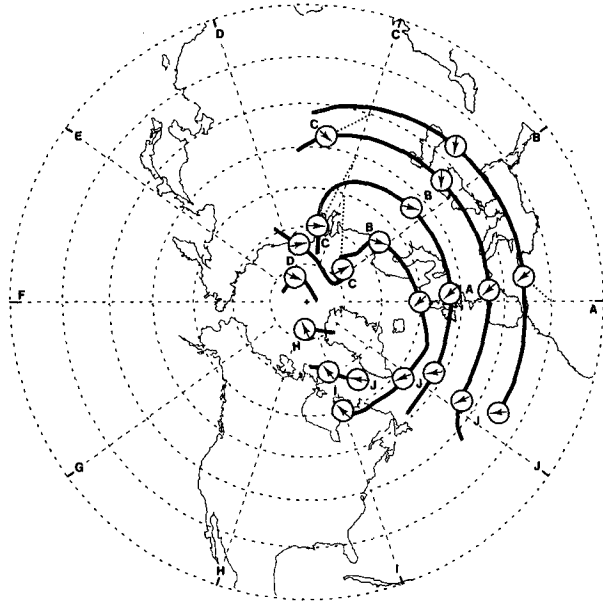


FIG. 7. As in Fig. 6, but with $\alpha_0 = -45^\circ$.

of the Alaskan high, where the flow is irregular and weak. Comparison with Fig. 4 indicates that the sudden warming has markedly reduced the ability of these waves to propagate vertically.

Equally significant, nevertheless, are the rather large areas still covered with these waves: 1) in the strongly curved flow near 90° ; 2) south of the low center, in what is basically a displaced and intensified polar night jet (no longer in the polar night, of course!); and 3) poleward of the Alaskan high. Due to the choice of a larger horizontal scale the reader will observe greater lateral movement of these rays in comparison to Fig. 4.

Figure 7 represents the same waves but having initial orientation

$$\alpha_0 = -45^\circ. \quad (4.4)$$

These waves propagate throughout the outer part of quadrant I (0 to 90°), but also in the strongly curved flow of upper quadrant IV and in a small region of quadrant I near the pole. Considerable cross-polar advection of waves is evident in Fig. 7 (compare Figs. 2b, c). For these waves, the flow in quadrants II and III is almost everywhere inimical to propagation.

Figures 6 and 7 indicate that large regions of the hemisphere are devoid of these two particular waves on this day. The question naturally arises as to whether these regions are devoid of all other quasi-stationary waves as well. The economical local method of Section 5 proved to be the easiest way to answer this question, at least for those waves expected to move rapidly in the vertical. Additionally some ray tracing simulations were done with other parameter combinations. In all of the simulations Lindzen's (1981) advice has been

followed: the ground-based phase speed is chosen to lie in the range of tropospheric flow speeds.

Figure 8 utilized the parameters

$$K_0 = 2\pi (50 \text{ km})^{-1}, \quad (4.5a)$$

$$\alpha_0 = 90^\circ, \quad (4.5b)$$

$$c = 0. \quad (4.5c)$$

These are meridional waves, such as might be due to any number of east-west mountain ranges (Himalayas, Alps, Brooks Range, Caucasus, etc.). Their propagation is generally hindered on this day, a notable exception being found in the polar cap where the basic flow is itself meridional. Also, there is some propagation west of the Alaskan high.

In an experiment with traveling waves (not shown) the following parameters were used:

$$K_0 = 2\pi (50 \text{ km})^{-1}, \quad (4.6a)$$

$$\alpha_0 = 0, \quad (4.6b)$$

$$c = -20 \text{ m s}^{-1}. \quad (4.6c)$$

Their zonal orientation implies zonal group and phase propagation in zonal winds, so that ray contour projections were found to lie virtually on top of their initial latitude circles. Overall their behavior reinforced what was said earlier about the stationary waves that propagate in westerlies south of the low and north of the high. Additionally, some propagation was observed for the traveling waves in the lower part of quadrant IV extending westward in quadrant III.

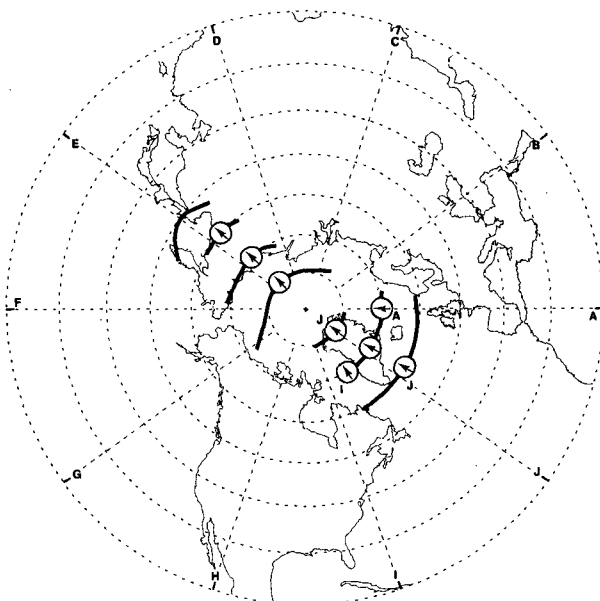


FIG. 8. As in Fig. 6, but with $K_0 = 2\pi (50 \text{ km})^{-1}$ and $\alpha_0 = 90^\circ$.

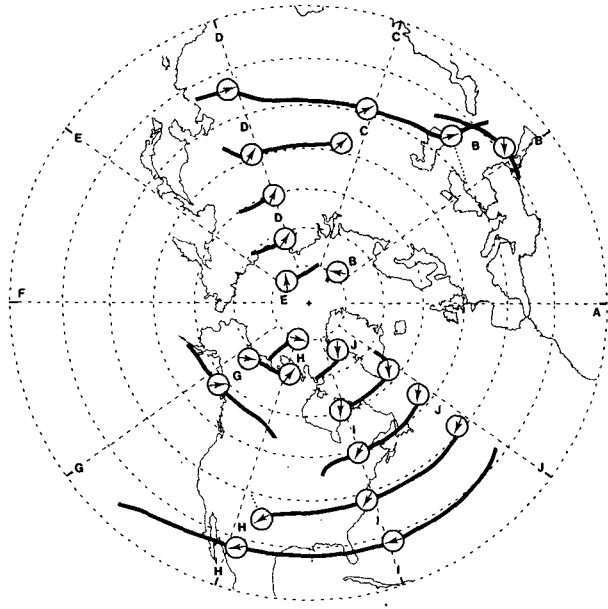


FIG. 9. As in Fig. 4, but for 22 February 1979.

c. 22 February 1979

Based on the results of the wave 1 warming, the results for 22 February 1979 were quite predictable; similar patterns were obtained, but having a wave 2 structure. Fig. 9 corresponds to the same wave parameters used in Fig. 4. A companion experiment was done with the parameters of Fig. 5 (not shown). Generally speaking, propagation of $+45^\circ$ (-45°) waves is favored to the southeast (southwest) of the cyclonic low centers. Propagation is slightly more favored over North America, however, due to the fact that the stratospheric mean flow is more equivalent barotropic there. (The less barotropic the flow, the greater the probability that a wave will encounter its critical level.)

Comparison to Figs. 4 and 5 demonstrates that gravity wave propagation to the mesosphere has been reduced, but hardly eliminated, by this major warming. Anticyclonic regions in Fig. 3 are characterized by weak winds (unlike the wave 1 warming where the anticyclonic westerly flow north of the Alaskan high allowed substantial wave propagation), but they cover less than half the hemisphere.

The reader will note a peculiar feature in Fig. 9, along the $60\text{--}240^\circ$ meridian at high latitudes. Here, winds are uniformly easterly throughout the stratosphere! More exactly, the mean flow is directed NE to SW, so that $+45^\circ$ waves are free to propagate vertically. An analogous situation appeared in the companion experiment (-45° waves) along the $120\text{--}300^\circ$ meridian, where mean winds are directed SE to NW. Whether such propagation would have been allowed by the tropospheric flow is unclear, but one should be careful to note that if propagation were allowed, the wave-induced mean flow acceleration due to these waves

would be directed opposite to its more usual orientation found in westerly flow. (Polar easterlies extending throughout the troposphere during a major warming may occur, though probably not very often. Note, however, that easterlies are not necessary in the excitation region; northerly flow over a NW-SE mountain range could, for example, excite waves having a nonzero westerly component of momentum flux.)

5. Matsuno's (1982) local approximation

a. Theory

Matsuno (1982) has discussed gravity waves of all orientation excited isotropically in the troposphere and propagating vertically in the middle atmosphere, but neglected their lateral movement and horizontal refraction. Although his model was zonally symmetric, this suggests a useful simplification valid for zonally asymmetric flows as well. Matsuno's approximation is therefore

$$\mathbf{u}_g \approx 0, \tag{5.1a}$$

$$d\mathbf{k}/dt \approx 0 \tag{5.1b}$$

(both horizontal vectors as in Section 2). Gravity waves are assumed to propagate straight up, more or less, and refraction in the horizontal wavevector is ignored.

The ray tracing results of Figs. 4-9 lend considerable justification to this approximation at the horizontal scales of interest here. To be sure, even at these scales a few highly displaced, horizontally refracted rays can always be found; however, their importance is likely to be minimal.

Matsuno (1982) then considered the transmissivity of waves in a diffusive flow, i.e.,

$$\tau(\mathbf{x}, \alpha_0) = \exp - \int_{z_0}^z \frac{2\nu m^2}{w_g} dz'. \tag{5.2}$$

Now the same thing could be done in a zonally asymmetric flow (including, for that matter, a scale-dependent radiative damping and/or wavebreaking); however, further simplification can be achieved for the intermediate-scale waves (for which the local approximation is most valid). Experience suggests that in many instances these waves either propagate directly to the mesosphere, or encounter their stratospheric critical level. In other words, for these waves stratospheric dissipative effects are generally weak away from critical levels. (Indeed, to the extent that the hydrostatic approximation remains valid, the integral in (5.2) can be made small away from the critical level by choice of large K .) For practical purposes, then, the transmissivity can be estimated in the following manner, valid for quasi-stationary waves:

$$\tau(\mathbf{x}, \alpha_0) \approx \begin{cases} 1 & \text{if } \mathbf{k}^* \cdot \bar{\mathbf{u}} \neq 0 \text{ in a column at } \mathbf{x} \text{ from } z_0 \text{ to } z, \\ 0 & \text{if } \mathbf{k}^* \cdot \bar{\mathbf{u}} = 0 \text{ in a column at } \mathbf{x} \text{ from } z_0 \text{ to } z. \end{cases} \tag{5.3}$$

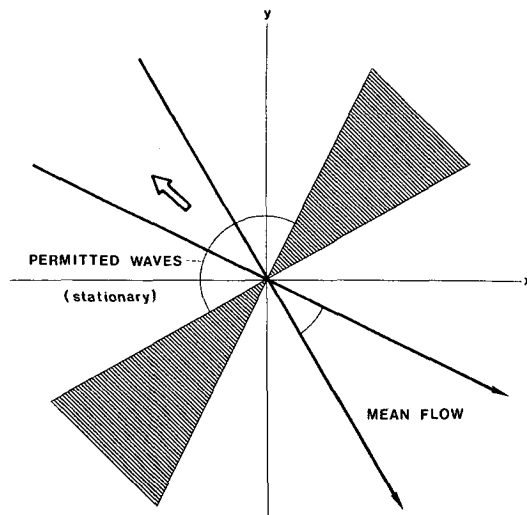


FIG. 10. Schematic diagram of how the average transmitted wavevector and the range of permitted wavevector orientations for stationary waves are obtained when the underlying mean flow orientation is known and Matsuno's approximation is assumed. As the wind vector rotates with height, orthogonal wavevectors are progressively removed.

Thus quasi-stationary waves that encounter their point of orthogonality or critical level are selectively absorbed, and all other orientations are freely transmitted.

Under quite general circumstances, it is possible to define the *average transmitted wavevector*³ in a column at x :

$$\langle \mathbf{k}^* \rangle \equiv \frac{\int_{-\pi/2}^{\pi/2} \tau(\mathbf{x}, \alpha_0) \text{sgn}(\hat{\omega}) \mathbf{k}^*(\alpha_0) B_0(\mathbf{x}, \alpha_0) d\alpha_0}{\int_{-\pi/2}^{\pi/2} B_0(\mathbf{x}, \alpha_0) d\alpha_0}, \tag{5.4}$$

$$\mathbf{k}^* \equiv \mathbf{i} \cos\alpha_0 + \mathbf{j} \sin\alpha_0, \tag{5.5}$$

where \mathbf{i} and \mathbf{j} are local unit vectors east and north, respectively, and $\mathbf{B}_0 \equiv B_0 \mathbf{k}^*$ is the momentum flux entering the stratosphere. When the integral is taken over the semicircle of possible orientations the sgn function insures that the wavevector convention is preserved (see footnote 2 above).

Equation (5.4) implies that for an isotropic excitation of stationary waves [$B_0 \equiv \text{constant}$, as assumed by Matsuno (1982)] and conservative flow away from critical levels the average transmitted wavevector lies midway between the mean flow orientation extrema in the underlying atmosphere, as shown in Fig. 10. Equivalently, it is directed midway between the ex-

³ This quantity represents the average nondimensional horizontal component of the total wavevector, independent of K when (5.3) and the comments immediately preceding are valid. Normalization is arbitrary.

trema of allowed wavevector orientations. The magnitude of the average transmitted wavevector is proportional to the bandwidth of allowed orientations, viz.,

$$|\langle k^* \rangle| = \frac{\sqrt{2}}{\pi} (1 - \cos \Delta \alpha)^{1/2}. \quad (5.6)$$

Equation (5.4) is, in effect, the appropriate generalization of selective transmission to three-dimensional flows, subject to Matsuno's approximation. There should be no difficulty, however, in understanding this natural extension from the two-dimensional flows that have been previously treated. For stationary waves, two-dimensional flow implies a critical level when the mean flow vanishes, whereas three-dimensional flow implies a critical level when the mean flow *in the direction of the wavevector* vanishes. Thus as the wind vector rotates with height (without necessarily approaching zero magnitude) waves orthogonal to the local mean flow are progressively eliminated through critical layer absorption.

Dissipation may take its toll on waves near the extrema of allowed orientation, of course, but this effect does not alter the fundamental result that to within Matsuno's approximation, *the average transmitted wavevector always lies within the range of wavevector orientations allowed by the underlying stratosphere.*

Although (5.4) has been referred to as a three-dimensional result, it could be more accurately described as a result for two-dimensional waves in a three-dimensional mean flow. Thus the direction of the net momentum flux $\mathbf{u}'\mathbf{w}'$ is given by the orientation of the

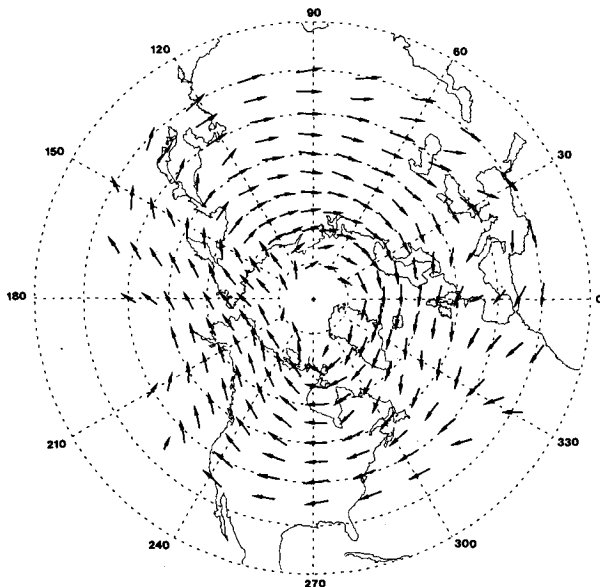


FIG. 11. Average transmitted wavevectors at 1 mb for 17 January 1979 assuming isotropic excitation and a conservative flow away from critical levels. For reference, the longest arrows, excluding arrowhead, are of maximum length $2\pi^{-1}$.

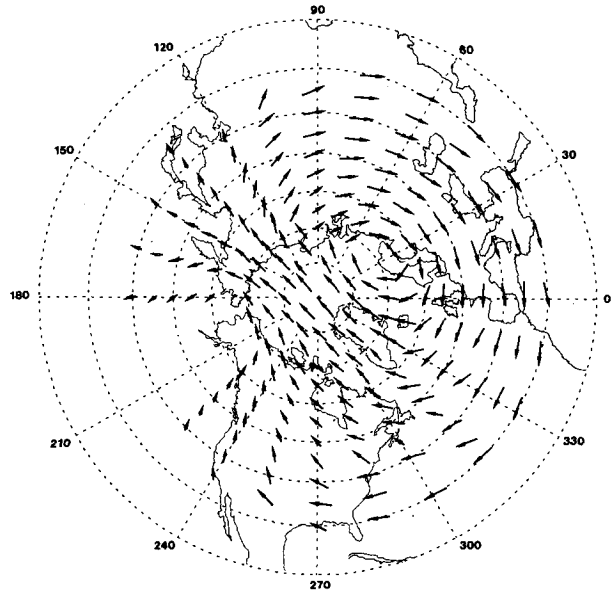


FIG. 12. As in Fig. 11, but for 26 January 1979.

average transmitted wavevector. Consequently, this vector determines the vertically-integrated wave-induced mean flow acceleration orientation in the overlying atmosphere. However, it is a nontrivial step to evaluate the local wave-induced mean flow acceleration, for this requires knowledge of the local divergence of the momentum flux, which will be determined by transience, wavebreaking, and dissipation. Nevertheless, irrespective of these effects, it is easy to show that to within Matsuno's approximation the local wave-induced mean flow acceleration will obey the same fundamental rule, always directed within the range of allowed orientations.⁴

b. Results obtained with Matsuno's approximation

Figure 11 shows the average transmitted stationary wavevectors at the 1 mb surface for 17 January 1979. It has been assumed that all orientations are excited isotropically, and that the motion is conservative away from the critical level. Thus Figs. 11–13 under these conditions indicate the following: (1) the bandwidth of allowed orientations determined by the magnitude of the average transmitted wavevector and Eq. (5.6); (2) the average orientation, i.e., the orientation midway between the extrema of allowed orientations; and (3) the direction of the net vertically-integrated (but not

⁴ Refraction in the horizontal wavevector complicates the mean flow acceleration, since momentum conservation clearly implies that \bar{u}_i is no longer aligned in the k -direction. Therefore the final orientations shown in Figs. 4–9 are not necessarily indicative of the body force acting on the overlying mesospheric flow, in the event that Matsuno's approximation is inaccurate due to the horizontal refraction (Dunkerton, 1984).

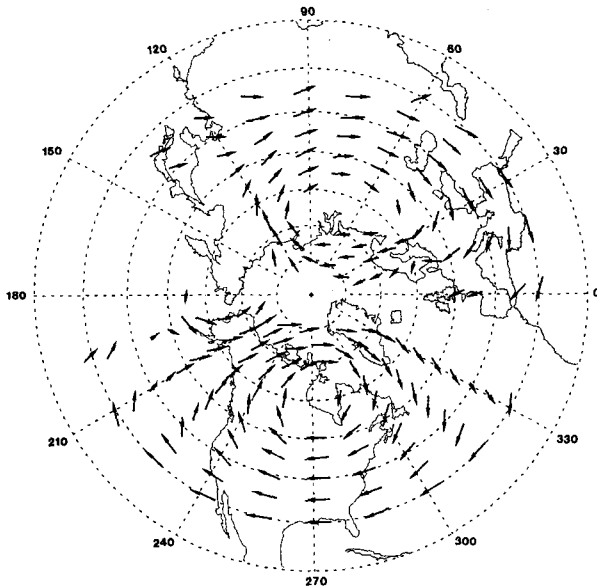


FIG. 13. As in Fig. 11, but for 22 February 1979.

local) wave-induced mean flow acceleration in the overlying atmosphere.

When it is accurate, as for waves of the intermediate range, Matsuno's approximation is an economical way to confirm and expand upon the ray tracing results. Immediately it becomes apparent which wavevector orientations are favored at a particular location. In general, wave propagation is favored to a greater degree in Fig. 11 than the ray tracing simulations suggested, because the latter incorporated dissipation. Nevertheless, Fig. 11 demonstrates that waves of several different orientations have no difficulty propagating vertically where the mean flow vector does not rotate with height. When the mean flow vector rotates with height, waves of orthogonal orientation are removed, creating a bias in the average orientation which is largely antiparallel to the mean flow. This confirms the results of Section 4a. For example, over western Canada the NW-SE bias is evident, as is the SW-NE bias over eastern Canada and eastern Siberia. A striking result is the degree to which waves are forbidden in the "Aleutian" high, and to a lesser extent, over part of Europe (dissipation would, of course, further inhibit propagation in and around these regions).

Figure 12 shows the corresponding pattern for the "minor" wave 1 warming of 26 January 1979. The antiparallel bias is even more evident, which is largely a tribute to the equivalent barotropy of the underlying flow. However, the reader will notice a distinct cross-streamline bias in the polar region which is attributable to the nonbarotropic alignment of the 100 mb flow (cf. Fig. 2a). At the pole, the average orientation lies roughly along the 120-300° meridian. Vertical propagation in the Alaskan high is even less evident now

that the warming has increased the magnitude and spatial extent of the anticyclonic flow.

Figure 13, finally, exhibits the wave 2 pattern for 22 February 1979. Note how the wavevectors exhibit a more circular pattern on the North American side, because the mean flow is more equivalent barotropic there. In the regions of easterly winds the antiparallel wavevector convention mandates that the arrows be drawn pointing, e.g., to the northeast over Alaska and to the southeast over Greenland—in both cases opposite to the prevailing mean flow.

6. Conclusion

Other effects being the same, sudden warmings are expected to reduce, but not eliminate, quasi-stationary gravity wave propagation to the overlying mesosphere. Selective transmission will produce significant local biases in the average wavevector orientation entering the mesosphere, due to critical layer absorption of orthogonal waves in the stratosphere. Lateral ray movement and horizontal refraction complicate this simple picture, but do not contradict it, at least for waves of the intermediate range. It is not yet entirely clear what effect a sudden warming will have on the larger-scale inertia-gravity waves. Presumably, there is an overall reduction of vertical gravity wave propagation at all scales when local easterlies appear and spread horizontally during the onset of a major warming. Evaluation of the net wave-induced mean flow acceleration in the overlying mesosphere, however, remains problematic even at the smaller scales for several reasons, including the anisotropy of excitation and the role of transience, wavebreaking, and dissipation. Moreover, it will be necessary to examine the mesospheric wind structure itself to determine the mean flow acceleration. Fortunately, there are considerable mesospheric data up to 0.1 mb for the time period examined in this paper; perhaps on this account progress can be made in understanding the mesospheric flow structure during these particular warmings.

It is noteworthy that the effect of sudden warmings on the mesosphere and lower thermosphere is gaining interest at the present time. Holton (1983) has noted that mesospheric cooling sometimes accompanies a stratospheric warming, which supposedly cannot be explained on the basis of the mean meridional advection arguments of Matsuno and Nakamura (1979). Holton (1983) attributes the cooling to radiative relaxation in the presence of reduced gravity wave drag. It is uncertain whether his model can properly evaluate the reduction in drag, however, because the gravity waves are assumed to "see" only the zonal mean wind profile. Holton's (1983) thesis is that the influence of gravity waves in the mesosphere above a sudden warming is felt via their absence; the gravity wave drag is completely removed when the zonal mean flow becomes easterly, and radiative relaxation occurs. As

noted in the Introduction, planetary waves complicate this simplistic view, because the zonally-averaged transmissivity generally differs from the transmissivity of waves in the zonal mean flow (Dunkerton, 1982b). Nevertheless, it is of interest to examine what extent Holton's (1983) thesis might be correct. Fig. 14 shows the zonally averaged zonal component of the average transmitted wavevector derived from Figs. 11-13. Propagation of zonal waves is attenuated north of about 75° on 26 January and north of about 60° on 22 February. By comparison, judging from the zonal mean zonal flow, the transmissivity of stationary zonal waves in the zonal mean flow would be zero north of about 60° on 26 January and north of about 55° on 22 February. Thus Holton's (1983) assumption if applied to these two warmings would have overestimated the reduction of gravity wave propagation in both cases, but more significantly so on 26 January (largely due to the propagation of waves north of the Alaskan high on this day). It remains to be seen whether this quantitative error would significantly affect Holton's (1983) theory of mesospheric cooling.

Potentially more significant is the fact that the mean flow acceleration will not be antiparallel to the mean flow in general. In Section 5 we have been careful to point out that the average transmitted wavevector gives the direction of the overlying vertically-integrated acceleration orientation without saying anything *per se* about the actual *local* acceleration orientation since the latter requires knowledge of transience, wave-breaking, and dissipation. It would be no small understatement to describe the evaluation of the local acceleration as a difficult and complicated problem.

The mean flow acceleration will generally have some nonzero component orthogonal to the mean flow itself, but it is difficult to explore this fact in more depth without submerging oneself in a morass of analytically intractable integrals, particularly if transience and dissipation are included. When the latter are neglected, as in Lindzen (1981), for example, it is possible to be a little more specific, although even here one is limited to a qualitative discussion apart from explicit numerical calculations. The simplest case appears to be that of the "small-amplitude continuum" in which we regard the mean flow acceleration as consisting of a delta-function spike associated with the critical level of Booker and Bretherton (1967) except that we consider an infinitesimal amount of wave action in each wavenumber orientation interval. In this case, the mean flow acceleration for stationary waves is finite at each height, and is *exactly* orthogonal to the mean flow (if it exists at all). The reason is that each small-amplitude stationary wave is depositing its momentum in the mean flow at its point of orthogonality, so that the acceleration is itself orthogonal to the local mean flow. Clearly there is an analogy with the Coriolis force; one might even say that the effect of stationary gravity waves in this case is to modify the Coriolis parameter, though in a complicated sort of way, dependent, among other things, on the lower-level flow and on the sense in which the wind vector rotates with height.

The small-amplitude continuum is of questionable relevance in the atmosphere since wavebreaking certainly occurs away from critical levels at least part of the time. It is precisely this fact (together with transience, dissipation and nonzero phase speeds) that al-

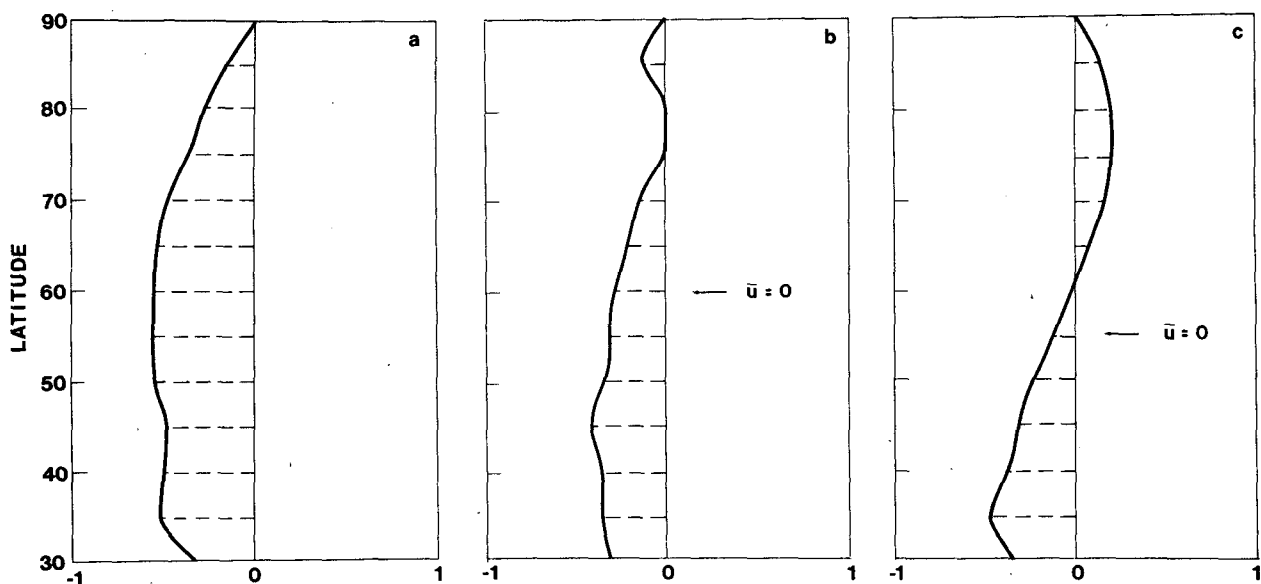


FIG. 14. Zonally averaged zonal component of the average transmitted wavevector for (a) 17 January 1979, (b) 26 January 1979 and (c) 22 February 1979. These profiles were obtained from the results shown in Figs. 11-13 by performing an Eulerian average of the zonal component of $\langle \mathbf{k}^* \rangle$ around a latitude circle.

lows a wave drag component antiparallel to the local mean flow. Once again restricting ourselves to Lindzen's (1981) steady, conservative waves model, we would find that convective wavebreaking occurs when

$$\left| B_0 \exp \frac{z}{H} \right| > \frac{1}{2} \left| \frac{K \bar{c}^3}{N} \right|. \quad (6.1)$$

For stationary waves, then, wavebreaking will occur for permitted waves outside of an angle α_r relative to the mean flow

$$\cos^3 \alpha_r \equiv \frac{2NB_0}{K|\bar{u}|^3} \exp(z/H). \quad (6.2)$$

Under isotropic excitation conditions waves of all possible orientation will break if the rhs of (6.2) is greater than unity. Even in this case we would generally find a component of the mean flow acceleration orthogonal to the local mean flow.

It might be argued that if one wave orientation begins to break, then all other orientations would undergo absorption as discussed by Matsuno (1982) and Holton (1982). The relevance of this argument depends on whether we are considering an ensemble of discrete wave events or the superposition of waves at a given time. In the latter case, we are led to suspect that the mean flow acceleration might tend to gravitate back towards the orientation of the average transmitted wavevector (antiparallel convention), though it would almost certainly be an oversimplification to expect the two vectors to coincide. Ultimately the mean flow acceleration, like the average transmitted wavevector, will be influenced by the anisotropy of wave excitation as well.

These theoretical difficulties reinforce the need for observational studies, not only of mesospheric planetary waves, but also of related problems. Kawahira (1983), for example, has recently discussed changes in D-region ionization during a sudden warming. On the basis of our results, caution should be exercised before attributing any such changes to gravity waves, even though Offerman *et al.* (1983) suggest that the D-region "winter-anomaly" may be associated with vertical eddy diffusion, possibly implying a gravity wave effect. Interestingly, Kawahira recognized the importance of planetary Rossby waves in the transport problem, underscoring the need for a careful analysis of warming-induced changes in wave transport at *all* scales.

Our theoretical results could, in fact, stimulate any number of observational studies. MST radars situated at various longitudes, for example, could determine whether significant changes in gravity wave propagation occur during a warming, which might be longitudinally-dependent. One such radar is currently in operation at Poker Flat, Alaska, and is ideally located for such a study, being in the region of anticyclonic flow during a major wave 1 warming as that of 26 January 1979. Closer to the surface, on the other hand,

our theoretical results suggest *regions of preferred stratospheric gravity wavebreaking* during a sudden warming. A global network of less expensive ST radars could examine such implications observationally.

Finally, there is clearly a need for studies of the mesospheric general circulation and a more detailed examination of possible effects of gravity waves or the lack thereof during a sudden warming, including effects on D-region ionization, mesospheric photochemistry, and planetary waves. This will require a cooperative effort among scientists of various disciplines. One problem of immediate interest to dynamical meteorologists is to determine what effect gravity waves have on planetary Rossby waves and vice versa. When the data become available, this question can be answered by examining the wind structure in the mesosphere above a warming, together with the sign of the Eliassen-Palm flux divergence due to planetary waves in this region (Andrews and McIntyre, 1976). Once the planetary wave structure is understood, the problem of wave transport in the mesosphere can then be addressed. Determining the relative roles of wave transport and sources and sinks for photochemical species and ionization in the mesosphere seems quite complicated at present. Indeed, all of these observational studies will be challenging but we hope rewarding in the coming years; the current understanding of mesospheric dynamics and transport, after all, can do nothing but improve.

Acknowledgments. Helpful conversations with D. C. Fritts, J. R. Holton, M. E. McIntyre and M. R. Schoeberl are gratefully acknowledged. Dr. Dunkerton's research was supported by the National Science Foundation, Grant ATM-8217503. Dr. Butchart was supported by the National Aeronautics and Space Administration, Grant NAG2-66.

REFERENCES

- Andrews, D. G., and M. E. McIntyre, 1976: Planetary waves in horizontal and vertical shear: The generalized Eliassen-Palm relation and the mean zonal acceleration. *J. Atmos. Sci.*, **33**, 2031-2048.
- Booker, J. R., and F. P. Bretherton, 1967: The critical layer for internal gravity waves in a shear flow. *J. Fluid Mech.*, **27**, 513-539.
- Bretherton, F. P., 1966: The propagation of groups of internal gravity waves in a shear flow. *Quart. J. Roy. Meteor. Soc.*, **92**, 446-480.
- Dunkerton, T. J., 1979: On the role of the Kelvin wave in the westerly phase of the semiannual zonal wind oscillation. *J. Atmos. Sci.*, **36**, 32-41.
- , 1980: A Lagrangian mean theory of wave, mean-flow interaction with applications to nonacceleration and its breakdown. *Rev. Geophys. Space Phys.*, **18**, 387-400.
- , 1982a: Wave transience in a compressible atmosphere, Part 3: The saturation of internal gravity waves in the mesosphere. *J. Atmos. Sci.*, **39**, 1042-1051.
- , 1982b: Stochastic parameterization of gravity wave stresses. *J. Atmos. Sci.*, **39**, 1711-1725.
- , 1984: Inertia-gravity waves in the stratosphere. Submitted to *J. Atmos. Sci.*

- , and D. C. Fritts, 1984: Transient gravity wave-critical layer interaction. Part I: Convective adjustment and the mean zonal acceleration. *J. Atmos. Sci.*, **41**, 992–1007.
- Fels, S. B., 1982: A parameterization of scale-dependent radiative damping rates in the middle atmosphere. *J. Atmos. Sci.*, **39**, 1141–1152.
- Gossard, E. E., and W. H. Hooke, 1975: Waves in the atmosphere. *Developments in Atmospheric Science*, Vol. 2, Elsevier, 456 pp.
- Holton, J. R., 1982: The role of gravity wave-induced drag and diffusion in the momentum budget of the mesosphere. *J. Atmos. Sci.*, **39**, 791–799.
- , 1983: The influence of gravity wave breaking on the general circulation of the middle atmosphere. *J. Atmos. Sci.*, **40**, 2497–2507.
- , and W. M. Wehrbein, 1980: A numerical model of the zonal mean circulation of the middle atmosphere. *Pure Appl. Geophys.*, **118**, 284–306.
- Jones, W. L., 1967: Propagation of internal gravity waves in fluids with shear flow and rotation. *J. Fluid Mech.*, **30**, 439–448.
- , 1969: Ray tracing for internal gravity waves. *J. Geophys. Res.*, **74**, 2028–2033.
- Kawahira, K., 1983: An observational study of the D-region winter anomaly and sudden stratospheric warmings. *J. Atmos. Terr. Phys.*, **44**, 947–956.
- Leovy, C. B., 1964: Simple models of thermally driven mesospheric circulations. *J. Atmos. Sci.*, **21**, 327–341.
- Lighthill, M. J., 1978: *Waves in Fluids*. Cambridge University Press, 504 pp.
- Lindzen, R. S., 1981: Turbulence and stress due to gravity wave and tidal breakdown. *J. Geophys. Res.*, **86C**, 9707–9714.
- Matsuno, T., 1982: A quasi one-dimensional model of the middle atmosphere circulation interacting with internal gravity waves. *J. Meteor. Soc. Japan*, **60**, 215–226.
- , and K. Nakamura, 1979: The Eulerian and Lagrangian mean meridional circulations in the stratosphere at the time of a sudden warming. *J. Atmos. Sci.*, **36**, 640–654.
- Offerman, D., H. G. K. Bruckelmann, J. J. Barnett, K. Labitzke, K. M. Torkar and H. U. Widdel, 1982: A scale analysis of the D-region winter anomaly. *J. Geophys. Res.*, **87**, 8286–8306.
- Schoeberl, M. R., and D. F. Strobel, 1978: The zonally averaged circulation of the middle atmosphere. *J. Atmos. Sci.*, **35**, 577–591.
- , and —, 1983: Nonzonal gravity wave breaking in the winter mesosphere. *Proc. Joint U.S.-Japan Conf. on the Middle Atmosphere*, J. R. Holton and T. Matsuno, Eds. Terrapub (in press).
- Smith, S., and D. C. Fritts, 1983: Estimation of gravity wave motions, momentum fluxes, and induced mean flow accelerations in the winter mesosphere over Poker Flat, Alaska. *Proc. 21st Conf. Radar Meteorology*, Edmonton, Amer. Meteor. Soc. (in press).
- Vincent, R. A., and I. M. Reid, 1983: HF Doppler measurements of mesospheric gravity-wave momentum fluxes. *J. Atmos. Sci.*, **40**, 1321–1333.